

# Numerical Analysis of Back Scattering from a Target over a Random Rough Surface Using DRTM

Kwang-Yeol Yoon

## Abstract

This paper is concerned with an analysis of the back scattering of electromagnetic waves from a target moving along random rough surfaces such as the desert, and sea. First, the discrete ray tracing method(DRTM) is introduced, and then, this method is applied to the back scattering problem in order to investigate the effect of the back scattering from random rough surfaces on the electric field intensities. Finally, numerical examples of various height deviations of the Gaussian type of rough surfaces are shown. It is numerically demonstrated that the back scattering is dominated by the diffractions related to the reflections from the random rough surfaces.

**Key words** : DRTM, Random Rough Surface, Backscattering Characteristics, Electromagnetic Wave Propagation.

## I . Introduction

Electromagnetic wave scattering by rough surfaces has attracted attention from the technical viewpoint of radar cross section associated with remote sensing technology<sup>[1],[2]</sup>. It is well known that flying objects just above a terrestrial surface are hardly detectable by radar installed on the surface. The objective of this paper is to numerically simulate a related problem where radar detects a target moving along a random rough surface. Back scattering of the electromagnetic waves emitted from the radar is caused mainly by the reflected waves from the target and the rough surface as well as the interacting reflections between them.

So far, the author has investigated two types of electromagnetic problems related to rough surfaces; the electromagnetic wave scattering from random rough surfaces, especially when the incident wave impinges upon them at a low grazing angle<sup>[2]</sup>, and the electromagnetic wave propagation along them<sup>[3]</sup>. In these investigations, the finite volume time domain(FVTD) method was used<sup>[4]</sup>. However, the method requires too much computer memory to deal with the larger area of rough surfaces than the wave length incident waves. Recently, different types of analytical and numerical methods have been proposed to deal with large size of random roughness compared with the wave length<sup>[5]~[7]</sup>. In this paper, the author first reviews the discrete ray tracing method (DRTM) to deal with electromagnetic wave propagation along rough surfaces. Next, the DRTM is applied to the electromagnetic wave back scattering from a target over a 1D rough surface. Finally, the back scattering charac-

teristics of a target flying just above the rough surface are investigated numerically.

## II . Discrete Ray Tracing Method

The geometry of the problem is shown in Fig. 1, where its structure is assumed to be one dimensional(1D). The height of the radar is the same as that of the target moving along the rough surface. It is assumed that the random rough surface is made of a lossy dielectric of which the electric property is specified by the dielectric constant  $\epsilon_r$  and conductivity  $\sigma$  and the target is composed of a perfect conductor. Random rough surfaces are numerically generated by the DFT method or the convolution method<sup>[3]</sup>. In the present simulation, only the Gaussian type of spectrum is considered for the rough

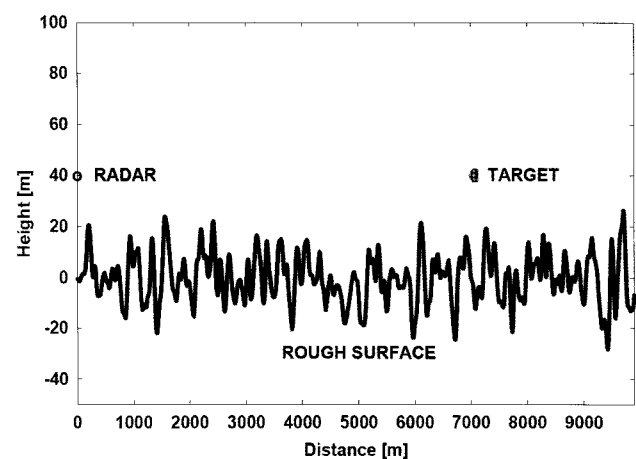


Fig. 1. Problem geometry.

Manuscript received April 29, 2010 ; revised May 25, 2010. (ID No. 20100429-008J)  
 Department of Electronic Engineering, Keimyung University, Daegu, Korea.

surfaces<sup>[2]</sup>. The spectrum density function is defined by  $W(K_i) = \frac{dv^2 cl}{2\sqrt{\pi}} e^{-K_i^2 cl^2 / 4}$ , where  $K_i$  is the angular frequency in space,  $dv$  is the root mean square surface height, and  $cl$  is the correlation length of the rough surface.

### 2-1 Discretization of the Rough Surface

The first step of the DRTM is to discretize a 1D rough surface in terms of straight lines so that it can be approximated by a piece wise linear line. It is important for the approximation that the computer memory requirement is as small as possible and the following discretization method is proposed. First, the  $x$ -axis is divided into  $n_x$  straight lines with length  $D_x$ . Then any types of rough surfaces can be discretized in terms of representative points as follows:

$$\rho_i = (x_i, H_1(x_i)) \quad (i = 0, 1, 2, \dots, n_x), \quad (1)$$

where

$$x_i = D_x(i) \quad (i = 0, 1, 2, \dots, n_x), \quad (2)$$

$H_1(x)$  is the height function of the 1D rough surface, and  $D_x$  is the length of each straight line in the  $x$ -direction. The height function of the rough surface is given numerically by the DFT method or convolution method<sup>[3]</sup>. Next the normal vectors of the discretized straight lines are derived by the following relations:

$$\mathbf{n}_i = (\mathbf{u}_z \times \mathbf{a}_i) / |\mathbf{u}_z \times \mathbf{a}_i| \quad (i = 0, 1, 2, \dots, n_x - 1), \quad (3)$$

where  $\mathbf{u}_z$  is the unit vector in the  $z$ -direction, and

$$\mathbf{a}_i = (\rho_{i+1} - \rho_i), \quad (4)$$

It should be noted that only the position vectors  $\rho_i$  and the normal vectors  $\mathbf{n}_i$  are enough to be used to search rays numerically for the 1D discretized rough surface. This fact results in a considerable simplification of the ray searching algorithm and it also saves computer memory.

### 2-2 Discrete Ray Tracing

The essence of the algorithm for searching rays by the proposed DRTM is summarized. It is assumed that the arbitrary two lines of the discretized rough surface are in line of sight(LOS), if a representative point of one straight line is in LOS with that of another line. Otherwise, they are not in line of sight(NLOS). In the present simulations, the representative point of a straight line has been chosen to be the starting point of the straight line, that is, at  $\rho_i$  in Eq. (1). This algorithm enables the

simplification of ray searching, resulting in great computation time savings. It is worth noting that the searched rays are approximate, but they can easily be modified to more accurate rays.

In the conventional ray tracing method(RTM), rays are classified into incident, reflection, and diffraction rays. In the present DRTM, however, they are divided into incident(source), source diffraction and image diffraction rays<sup>[7]</sup>. The source diffraction is the diffraction of the incident wave or source wave, and it is classified into two types a source diffraction in the illuminated region if the representative point of the straight line is in LOS, and a source diffraction in the shadow region if it is in NLOS. The present DRTM considers only the source diffraction rays with the shortest path from the source to the receiver. Thus, the source diffraction rays are constructed so that the representative points in LOS or NLOS may form the shortest path from the source to the receiver.

The image diffraction rays are closely related to the reflection rays which can be described in terms of geometrical optics as emitted waves from the images of a source or their diffraction at the edges of their own straight lines. Image diffraction rays can be successively constructed by connecting two different lines using representative points, if they are in LOS. It should be noted that the conventional reflection rays are included in the present image diffraction rays as a special type of rays that satisfy the Snell's law or the condition of the incident and reflection angles being equal. Fig. 2 shows a numerical example of traced rays. The radar is placed at  $x=0$  m and  $y=40$  m and the head of the target is at  $x=7$  km and  $y=40$  m. The length of the rough surface is 10 km and its parameters are chosen as  $cl=50$  m and  $dv=10$  m. The target model was supposed as a missile and the length of the target from head to tail was 100 m.

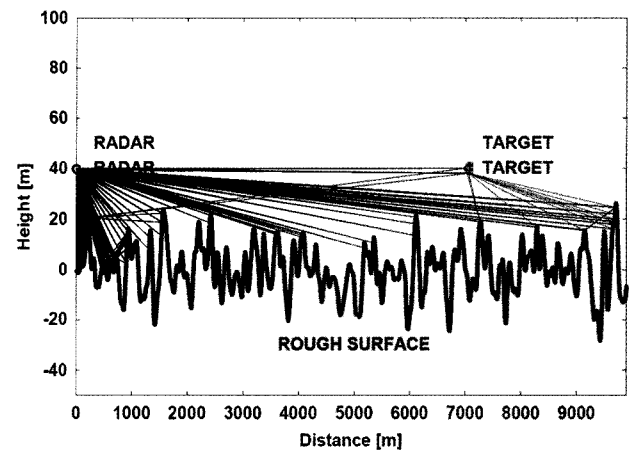


Fig. 2. Ray examples.

### 2-3 Field Computations

Fig. 3 shows the incident and reflected waves at a plane. The incident wave is described as a source field since it emits from a source, and the reflected wave is expressed as an image field since it behaves as though it emits from the image of the source. The received fields are expressed for E-wave and H-wave as follows:

$$E_z = E_z^s + R^e(\theta)E_z^i, \quad H_z = H_z^s + R^h(\theta)H_z^i, \quad (5)$$

where

$$E_z^s, H_z^s = \frac{e^{-j\kappa r_0}}{r_0}, \quad E_z^i, H_z^i = \frac{e^{-j\kappa r}}{r}, \quad (6)$$

where  $r = r_1 + r_2$ ,  $\kappa = \omega\sqrt{\epsilon_0\mu_0}$ ,  $E_z^s$ , and  $H_z^s$  are source or incident waves, and  $E_z^i$  and  $H_z^i$  are image or reflection waves. Reflection coefficients for horizontal and vertical polarizations are given by

$$R^h(\theta) = \frac{\cos\theta - \sqrt{\epsilon_c - \sin^2\theta}}{\cos\theta + \sqrt{\epsilon_c - \sin^2\theta}}$$

$$R^v(\theta) = \frac{\epsilon_c \cos\theta - \sqrt{\epsilon_c - \sin^2\theta}}{\epsilon_c \cos\theta + \sqrt{\epsilon_c - \sin^2\theta}},$$

$$\epsilon_c = \epsilon_r - j \frac{\sigma}{\omega\epsilon_0} \quad (7)$$

where  $\theta$  is the incident angle,  $\epsilon_r$  is the dielectric constant, and  $\sigma$  is the conductivity of the rough surface medium.

Now the source diffraction shown in the Fig. 4 is considered. It is assumed here that the electromagnetic fields due to the source diffraction can be approximated by the Wiener-Hopf solutions to the plane wave diffraction by a perfectly conducting semi-infinite half plane. The field expressions for H-wave are omitted for brevity, and the results are summarized as follows:

$$E_z = \begin{cases} E_z^s - D(r_2, \theta)E_z^d & \text{(Region I)} \\ D(r_2, \theta)E_z^d & \text{(Region II)} \end{cases}, \quad (8)$$

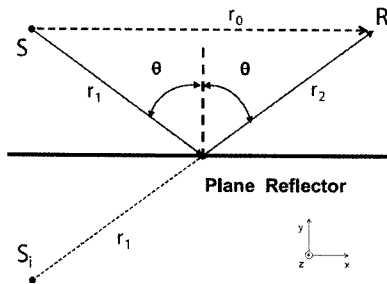


Fig. 3. Incident and reflected waves.

where the diffraction field is given by

$$E_z^d = \frac{e^{-j\kappa r}}{r}, \quad r = r_1 + r_2 \quad (9)$$

and the diffraction coefficient is given by

$$D(r_2, \theta) = e^{jX^2} F(X), \quad X = \sqrt{\kappa r_2(1 - \cos\theta_2)}. \quad (10)$$

The complex type of Fresnel function is defined by

$$F(X) = \frac{e^{\frac{\pi}{4}j}}{\sqrt{\pi}} \int_X^\infty e^{-ju^2} du \quad (X > 0), \quad (11)$$

This function has the following analytical properties:

$$F(X) = 1 - F(-X) \quad (X < 0)$$

$$F(X) \approx \frac{e^{-\frac{\pi}{4}j}}{2\sqrt{\pi}X} e^{-jX^2} \quad (X \gg 1) \quad (12)$$

Finally the image diffraction shown in Fig. 5, where the space is divided into three parts Region I, II and III is considered. In this case, the image diffraction coefficients can be summarized as follows:

$$E_z = \begin{cases} R^h(\theta)D(r_{12}, \theta_1)E_z^{d_1} - R^h(\theta)D(r_{22}, \theta_2)E_z^{d_2} & \text{(I)} \\ E_z^s - R^h(\theta)D(r_{12}, \theta_1)E_z^{d_1} - R^h(\theta)D(r_{22}, \theta_2)E_z^{d_2} & \text{(II)} \\ R^h(\theta)D(r_{22}, \theta_2)E_z^{d_2} - R^h(\theta)D(r_{12}, \theta_1)E_z^{d_1} & \text{(III)} \end{cases}, \quad (13)$$

where

$$E_z^{d_1} = \frac{e^{-j\kappa r_1}}{r_1}, \quad E_z^{d_2} = \frac{e^{-j\kappa r_2}}{r_2},$$

$$r_1 = r_{11} + r_{12}, \quad r_2 = r_{21} + r_{22} \quad (14)$$

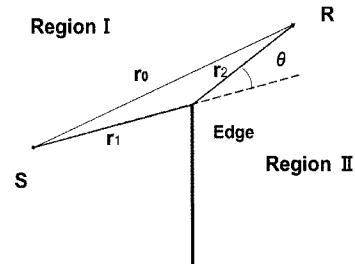


Fig. 4. Source diffraction.

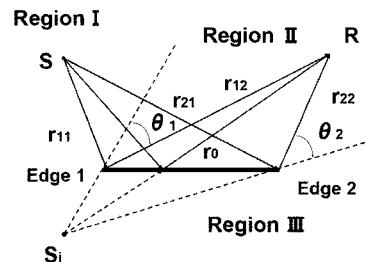


Fig. 5. Image diffraction by a plate.

It should be noted that the conventional reflection ray is included in the image diffraction ray in Region II, resulting in simplification of the proposed DRTM.

The principle of the DRTM algorithm has been discussed for the approximate evaluation of the electric field. The electric field  $E$  at the receiver is formally expressed in the following dyadic and vector form:

$$E = \sum_{n=1}^N \left[ \prod_{m=1}^{M_n^i} (D_{nm}^i) \cdot \prod_{k=1}^{M_n^s} (D_{nk}^s) \cdot E_0 \right] \frac{e^{-j\kappa r_n}}{r_n}, \quad (15)$$

where  $E_0$  is the electric field of the  $n$ -th ray at the first reflection or diffraction point, and  $\kappa$  is the wave number in the free space.  $N$  is the total number of rays considered,  $M_n^s$  is the number of source diffractions times, and  $M_n^i$  is the number of image diffractions times. Based on the ray data, the distance of the  $n$ -th ray from the source to the receiver is given by

$$r_n = \sum_{k=0}^{k=M_n^i+M_n^s} r_{nk} \quad (n=1,2,\dots,N), \quad (16)$$

where  $r_{nk}$  is the  $k$ -th distance from one reflection or diffraction point to the next.

### III. Numerical Results

Figs. 6~9 show numerical examples of back scattered electric field intensities versus distance between the radar and the target for rough surfaces with different target heights at  $h=40$  m, 100 m, 500 m, and 1,000 m, respectively. These curves are the ensemble average of electric field intensities computed by using 50 generated samples of rough surfaces. The dielectric constant of the flat ground is  $\epsilon_r=5.0$ , conductivity is  $\sigma=0.0023$ , and the

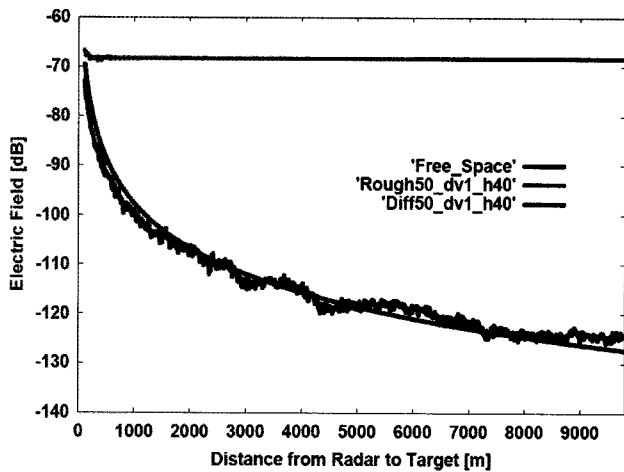


Fig. 6. Back scattering for the rough surface( $dv=1$  m,  $cl=50$  m and  $h=40$  m).

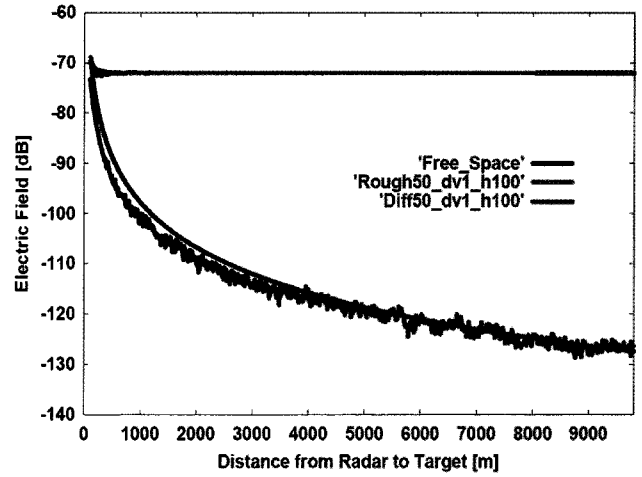


Fig. 7. Back scattering for the rough surface( $dv=1$  m,  $cl=50$  m and  $h=100$  m).

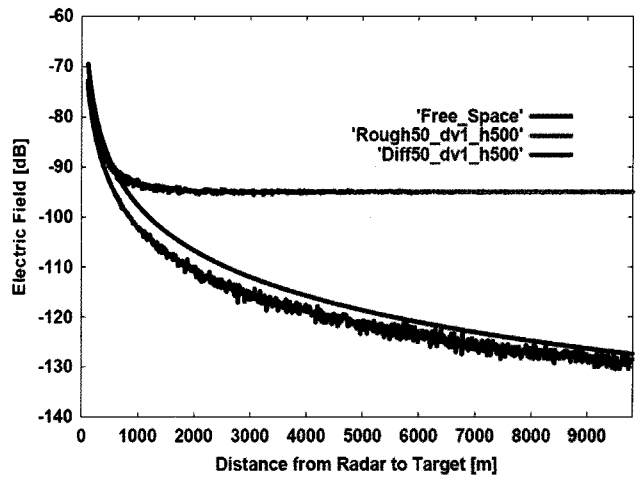


Fig. 8. Back scattering for the rough surface( $dv=1$  m,  $cl=50$  m and  $h=500$  m).

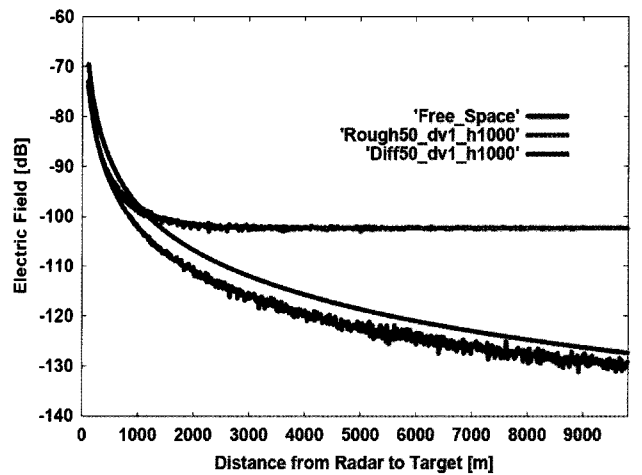


Fig. 9. Back scattering for the rough surface( $dv=1$  m,  $cl=50$  m and  $h=1,000$  m).

target is made of a perfect conductor. The length of the rough surface is 10 km and its parameters are chosen as  $cl=50$  m and  $dv=1$  m. The operating frequency is chosen as  $f=1$  GHz. In these figures, three curves are plotted: 1) the electric field of back scattering in case of free space (Free\_Space), 2) the back scattering of the total field (Rough50), that is, the back scattering from the rough surface plus the back scattering from the target, and 3) the electric field from the target (Diff50), that is, the total field minus the back scattered field due to the rough surface. It is demonstrated that the back scattering from the rough surface is very strong compared with that from the target.

Figs. 10 and 11 show numerical examples of back scattered electric field intensities versus distance between the radar and the target, with a target height of 100 m for different height deviations of the rough surface. These curves depict the ensemble average of the electric field

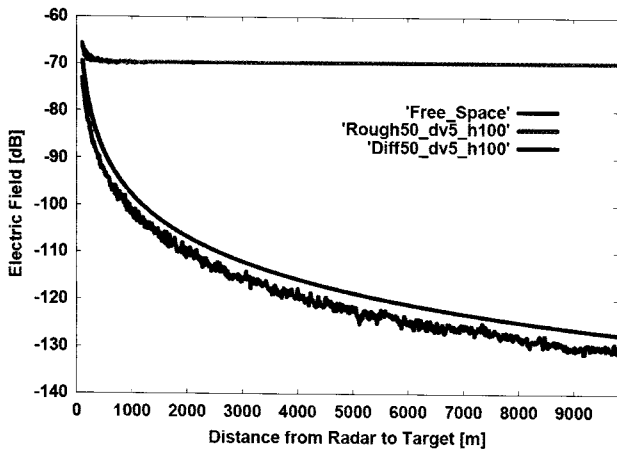


Fig. 10. Back scattering for the rough surface( $dv=5$  m,  $cl=50$  m and  $h=100$  m).

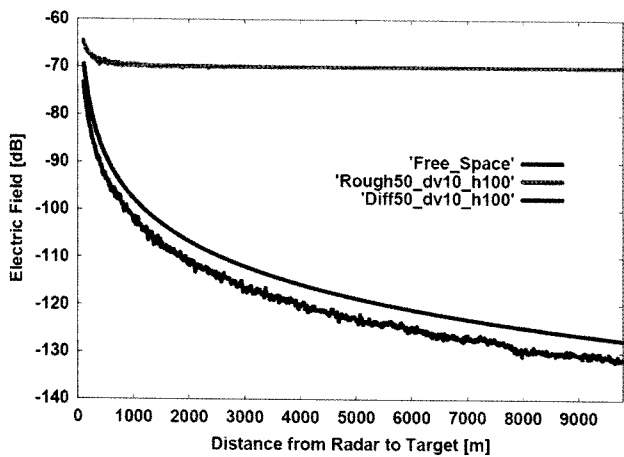


Fig. 11. Back scattering for the rough surface( $dv=10$  m,  $cl=50$  m and  $h=100$  m).

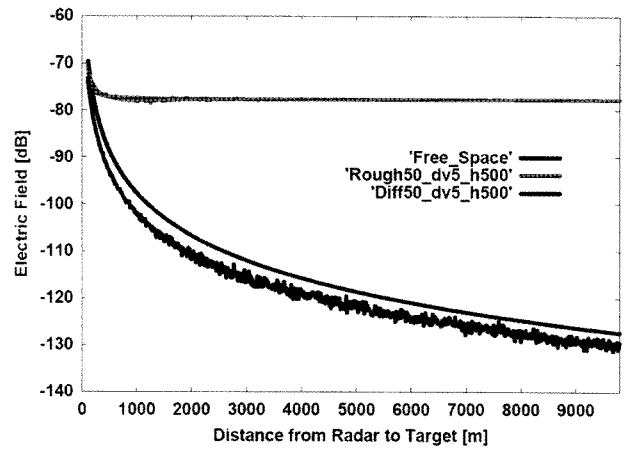


Fig. 12. Back scattering for the rough surface( $dv=5$  m,  $cl=50$  m and  $h=500$  m).

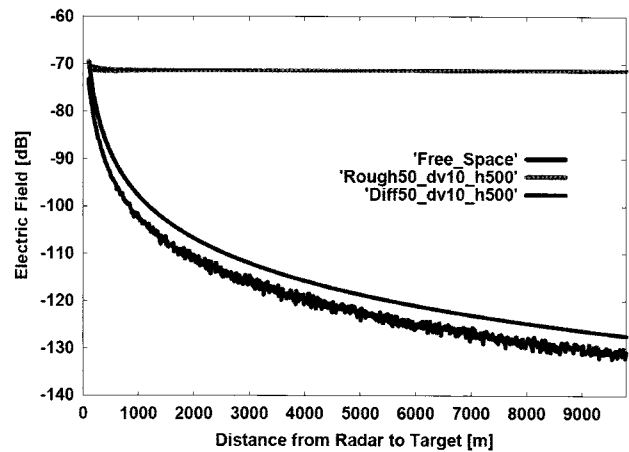


Fig. 13. Back scattering for the rough surface( $dv=10$  m,  $cl=50$  m and  $h=500$  m).

intensities computed by using 50 generated samples of rough surfaces. Material constants and the operating frequency are the same as in the former examples. The three curves also denote the same physical meaning as the former examples and it is demonstrated that the back scattering from the rough surface is very strong compared with that from the target.

Figs. 12 and 13 show numerical examples of back scattered electric field intensities versus distance between the radar and the target, with the target height at  $h=500$  m for different height deviations of the rough surfaces  $dv=5$  m and 10 m. It is also demonstrated that the back scattering from the rough surface is very strong compared with that from the target.

#### IV. Conclusion

This paper has introduced DRTM for numerical analyses

of the back scattering of electromagnetic waves from a target moving along random rough surfaces. The intention of the present method is to discretize not only a rough surface, but also the ray tracing procedure.

Numerical calculations were carried out for a 1D rough surface with different height deviations. It was shown that the back scattering from rough surfaces dominates the total back scattering and the difference field of the back scattering is lowered in comparison with the back scattering from a target in the free space. Modification of the present DRTM to 2D random rough surfaces deserves future investigation.

This work was supported by the Ministry of Knowledge Economy(MKE) and Korea Institute for Advancement of Technology(KIAT) through the Center for Mechatronics Parts(CAMP) at Keimyung University.

### References

- [1] E. I. Thoros, "The validity of the Kirchhoff approximation for rough surface scattering using a Gaussian roughness spectrum", *J. Acoust. Soc. Am.*, vol. 83, no. 1, pp. 78-92, Jan. 1988.
- [2] K. Y. Yoon, M. Tateiba, and K. Uchida, "FVTD simulation for random rough dielectric surface scattering at low grazing angle", *IEICE Trans. Electron.*, vol. E83-C, Dec. 2000.
- [3] K. Uchida, H. Fujii, M. Nakagawa, X. F. Li, and H. Maeda, "FVTD analysis of electromagnetic wave propagation along rough surface", *IEICE Trans. Commun.*, vol. J90-B, no. 1, pp. 48-55, Jan. 2007.
- [4] K. Y. Yoon, "Scattering characteristic from building walls with periodic and random surface", *Tran. KEES*, vol. 15, no. 4, pp. 428-435, 2004.
- [5] P. D. Holm, "Wide-angle shift-map pe for a piecewise linear terrain - A finite difference approach", *IEEE Trans. Antennas Propag.*, vol. 55, no. 10, pp. 2773-2789, Oct. 2007.
- [6] N. Dechamps, C. Bourlier, "Electromagnetic scattering from a rough layer: Propagation-inside-layer expansion method combined to an updated BMIA/CAG approach", *IEEE Trans. Antennas Propag.*, vol. 55, no. 10, pp. 2790-2802, Oct. 2007.
- [7] K. Uchida, H. Fujii, M. Nakagawa, J. Honda, and K. Y. Yoon, "Analysis of electromagnetic wave propagation along rough surface by using discrete ray tracing method", *Proceedings of ISAP 2008*.

### Kwang-Yeol Yoon



received B.E. and M.E. degrees from Fukuoka Institute of Technology, Fukuoka, Japan, in 1994, and 1996, respectively, and a D.E. degree in computer science and communication engineering in 2001 from Kyushu University, Japan. Since 2001, he has been an associate professor of the department of electronic engineering at

Keimyung University, Korea. He is a member of IEICE of Japan and the KEES of Korea. His main interests are in electromagnetic wave scattering from a rough surface.